Diffraction of beams by Ronchi rulings: comparison between two methods for gaussian spot size measurements

A. Ortiz-Acebedo, O. Mata-Mendez, and F. Chavez-Rivas
Departamento de Física, Escuela Superior de Física y Matemáticas, Instituto Politécnico Nacional, 07738 Zacatenco, Distrito Federal, México,
e-mail: omatax@yahoo.com

D. Hernández-Cruz and Roger A. Lessard
Center of Optics, Photonics and Lasers. Department of Physics, Engineering Physics and Optics, Laval University. Quebec (Quebec) G1K 7P4, Canada.

Recibido el 29 de noviembre de 2006; aceptado el 28 de marzo de 2007

Two independent methods for Gaussian spot size measurement are experimentally compared. The two methods use a Ronchi ruling where the transmitted total power and the normally diffracted energy are considered. We show that the beam widths obtained by these methods are very close. The theory of diffraction used is based on the Rayleigh-Sommerfeld integral equation with Dirichlet condition.

Keywords: Diffraction; gratings; Ronchi rulings.

Comparamos experimentalmente dos métodos para la determinación del ancho de una haz gauseano. Los dos métodos emplean una red de difracción de Ronchi donde se considera la energía total transmitida y la energía difractada normalmente. La teoría de la difracción utilizada esta basada en la ecuación integral de Rayleigh-Sommerfeld con las condiciones de Dirichlet.

Descriptores: Difracción; redes de difracción; redes de Ronchi.

Descriptores: Difracción; redes de difracción; redes de Ronchi.

PACS: 42.25.Fx; 42.10.H.C

1. Introduction

For most applications, the size to which a laser beam can be focused is an important fact. For instance, the optical data storage in compact discs requires beams with a 1-μm diameter[1]. Several methods for measuring Gaussian beam diameters have been proposed[2-5]. For 0.6-mm or longer Gaussian beam diameters, experimental comparisons among the scanning knife edge method, the scanning slit method, a method based on the second moment or variance, and the so called TEM_{00} method have been considered by Wright[3], with the conclusions that although these methods do not produce identical results they are sufficiently close.

Some other interesting and powerful theoretical methods have been proposed, based on the properties of the light transmitted by rulings. Thus, Ronchi rulings[6] (grating with alternate transparent and opaque regions per period) could be used to estimate the 1/e Gaussian beam radius r_0, as long as $0.2 < r_0/d < 1.2$, where d is the period of the ruling. The lower or upper limits fixed by Ronchi rulings are considerable improved by means of Ronchi-sinusoidal[6,7], Ronchi-triangular[6,7], periodic exponential rulings[8,9], and aperiodic gratings[10].

In all the above mentioned techniques using rulings[6-10] the beam diameters have been determined by means of the maximum and the minimum transmitted power. However, an exception is given in Ref. 11, where two different methods based directly on the diffraction properties of Gaussian beams through a lamellar grating have been proposed. In the first method, attention is focused on the normally diffracted energy to the grating at maximum and minimum transmitted power. In the second one, the beam diameter is obtained from the angular position of the first minimum of the diffraction pattern determined at minimum transmitted power. In passing we mention that, to our knowledge, the first time that the normally diffracted energy was proposed in order to determine the width spot of Gaussian beams was in Ref. 4, where a single slit was used, and this method was experimentally tested in Ref. 12.

Experimental comparisons between two different methods based on Ronchi rulings are given. One method considers the transmitted power, and the other one the normally diffracted energy to the ruling, both of them under conditions of maximum and minimum transmitted power. The theory of diffraction is obtained from the two-dimensional Rayleigh-Sommerfeld integral equation[4,11,13,14] with Dirichlet conditions; this theory can be applied to the cases of Gaussian beams, Hermite-Gaussian beams, and to other general beams.

2. Diffraction theory

We have a ruling made of alternate transparent and opaque zones. The period of the ruling is $d = \ell_1 + \ell_2$, where ℓ_1 is the width of the opaque zone and ℓ_2 the width of the transparent zone. We fixed a cartesian coordinate system with the Oz-axis parallel to the ruling as shown in Fig. 1. The ruling is illuminated by a beam wave independent of the z

coordinate (cylindrical incident wave). The time dependence $\exp(-i\,\omega\,t)$ is used and omitted in the following explanation.

Let $E(x)$, $E_i(x)$, and $t(x)$ be the transmitted field, the input field or incident field, and the grating transmittance function, respectively, related as follows:

$$E(x) = t(x)E_i(x). \tag{1}$$

From this equation, the field $E(x)$ just below the ruling can be obtained. Since we are interested in incident beam waves of finite cross section, then the function $E(x)$ will be different from zero within a finite interval $[a, b]$ and zero outside it (or very close to zero). The function $t(x)$ is null in the opaque zones, and has the unit value in the transparent zones. However, it is interesting to note that the theory presented in this paper can be utilized not only for the particular case of Ronchi rulings but also for holographic gratings.

From the field $E(x)$, it is possible, by means of the two-dimensional Rayleigh-Sommerfeld integral equation [4,11,13,14] with Dirichlet conditions, to get the total field $E(x_0, y_0)$ at any point (x_0, y_0) below the grating

$$\begin{aligned} E(x_0, y_0) &= \frac{i}{2}\int_{-\infty}^{\infty} E(x)\frac{\partial}{\partial\, y_0}H_0^1(kr)dx \\ &= \frac{i}{2}\int_{-\infty}^{\infty} t(x)E_i(x)\frac{\partial}{\partial\, y_0}H_0^1(kr)dx, \end{aligned} \tag{2}$$

where $k = 2\pi/\lambda$, with λ the wavelength of the incident radiation, $r^2 = (x - x_0)^2 + y_0^2$ with $P(x_0, y_0)$ the observation point as illustrated in Fig. 1, and H_0^1 is the Hankel function of the first kind and order zero.

From Eq. (2), the far field can be obtained by looking at the asymptotic behavior of the field E when $kr \gg 1$. In this approximation, the Hankel function is given by

$$H_0^1(kr) \approx \sqrt{2/\pi\, kr}\ \exp(i\pi\,/4)\exp(ikr); \tag{3}$$

then, the partial derivative in Eq. (2) is given by

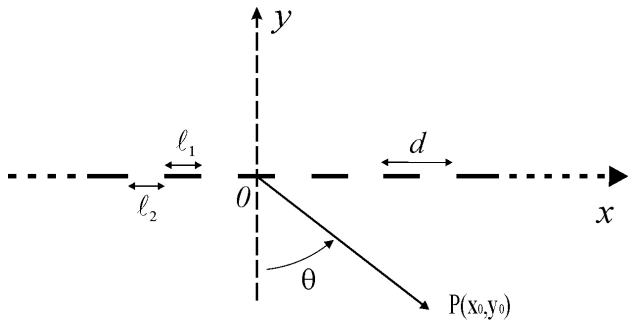

FIGURE 1. A Ronchi ruling made of alternate opaque and transparent zone of widths ℓ_1 and ℓ_2, respectively. The slits are parallel to the Oz axis.

$$\begin{aligned} &\frac{\partial}{\partial\, y_0}H_0^1(kr) \\ &\quad\approx -i\sqrt{2k/\pi}\exp(-i\pi/4)\frac{\exp[ik(r_0 - x\sin\theta)]}{r_0^{1/2}}\cos\theta; \end{aligned} \tag{4}$$

where for our ruling we have used $r \approx r_0$ in the denominator, $r \approx r_0[1 - (xx_0/r_0^2)]$ in the exponential, $\sin\theta = x_0/r_0$, and $\cos\theta = -y_0/r_0$ (see Fig. 1). It is important to note that, in taking the partial derivative of Eq. (3), we have retained the $1/r^{1/2}$ term and neglected the $1/r^{3/2}$ term. After substituting Eq. (4) into Eq. (2), we get the expression for the far field

$$E(x_0, y_0) = f(\theta)\exp(ikr_0)/\sqrt{r_0}, \tag{5}$$

which is the expression of a cylindrical wave with the oblique factor $f(\theta)$ given by:

$$f(\theta) = \sqrt{k}\exp(-i\pi/4)\cos\theta\ \hat{E}(k\sin\theta), \tag{6}$$

with $\hat{E}(\alpha)$ the Fourier transform of $E(x)$

$$\begin{aligned} \hat{E}(\alpha) &= \frac{1}{\sqrt{2\pi}}\int_{-\infty}^{+\infty} E(x)\exp(-i\alpha\, x)dx \\ &= \frac{1}{\sqrt{2\pi}}\int_{-\infty}^{+\infty} t(x)E_i(x)\exp(-i\alpha\, x)dx \end{aligned} \tag{7}$$

From the oblique factor $f(\theta)$ given in Eq. (6), we can obtain the total field $E(x_0, y_0)$ at any point (x_0, y_0) below the grating by means of Eq. (5). The intensity $I(\theta)$ scattered at an angle θ (see Fig. 1) is given by $C\,|f(\theta)|^2$, where C is a constant which will be taken as unity since we are interested only in relative quantities, so that we have

$$I(\theta) = \frac{1}{2\pi}k\cos^2\theta\left|\int_{-\infty}^{+\infty} t(x)E_i(x)\exp(-ik\sin\theta x)dx\right|^2. \tag{8}$$

In the following explanation, our attention is focused on the transmitted power P_T and on the intensity $I(0^0)$ diffracted normally to the screen, which will be denoted by E. The normally diffracted energy E by the ruling is calculated from Eq. (8) by

$$E = \frac{k}{2\pi}\left|\int_{-\infty}^{+\infty} t(x)E_i(x)dx\right|^2, \tag{9}$$

and the transmitted power P_T is obtained as follows:

$$P_T = \int_{-\pi/2}^{\pi/2} I(\theta)d\theta \tag{10}$$

3. Some applications

3.1. Incident Hermite-Gaussian beams

As an application of the results given above, we now consider the particular case of an incident Hermite-Gaussian beam on a Ronchi ruling of period $d = \ell_1 + \ell_2$, where ℓ_1 is the width of the opaque zone and ℓ_2 the width of the transparent zone. For Hermite-Gaussian beams at oblique incidence θ_i, the spectral amplitude $A(\alpha)$ is given by [11]

$$A(\alpha) = \frac{L}{2}(i)^m H_m\left[-\frac{L}{2}q_1(\theta_i)\right] q_2(\theta_i) \times \exp\left[i(-\alpha b + \beta h)\right] \exp(-q_1(\theta_i)^2 L^2/8), \quad (11)$$

where

$$q_1(\theta_i) = \alpha\cos\theta_i - \beta\sin\theta_i$$

and

$$q_2(\theta_i) = \cos\theta_i + (\alpha/\beta)\sin\theta_i.$$

The position of the incident Hermite-Gaussian beam with respect to the Oy axis is fixed by the parameter b. This parameter enables us to displace the beam wave along the screen. We denote by L the local $1/e$-intensity Gaussian beam diameter (the L-spot diameter). The coordinates (b, h) fix the position of the beam waist. These Hermite-Gaussian beams can be experimentally generated by means of end-pumped solid-state lasers [15].

In Fig. 2, the diffraction patterns of Hermite-Gaussian beams is plotted at the angle of incidence $\theta_i = 30°$, for $m = 1, 2$. The parameters used are ℓ_1=0.5, $\ell_2 = 1.0$, $L = 10/\sqrt{2}$, $\lambda = 0.1$, and the position of the center of the beam waist is fixed at the point (b, h)=(20.0,4.0). It is interesting to compare these results for a Ronchi ruling with those given in Fig. 7 of Ref. 14 where the diffraction of Hermite-Gaussian beams for a slit were considered.

The diffraction pattern of Fig. 2 shows the typical orders resembling those of the diffraction of plane waves by a grating, except that these are wider. We compared the angular positions of the orders seen in Fig. 2 with those calculated directly from the grating equation and a very good agreement was found. In fact, if we denote by n the several orders, by N our numerical results, and by GE the results obtained by means of the grating equation, we have $(n, N, GE) = (-4, 13.5, 13.49)$, (-2, 21.50, 21.51), (-1, 25.66, 25.67), (0, 30, 30), (1, 34.53, 34.51), (2, 39.30, 39.29), (4, 50.04, 50.05). We note that at the maxima (orders), one dip appear for $m = 1$ and two dips appear for $m = 2$; in the general case m dips appear at the maxima for a given m.

3.2. 3.2 Influence of the transparent and opaque zones

Now we go to consider the intensity ratio K defined as

$$K = E_{\min}/E_{\max}, \quad (12)$$

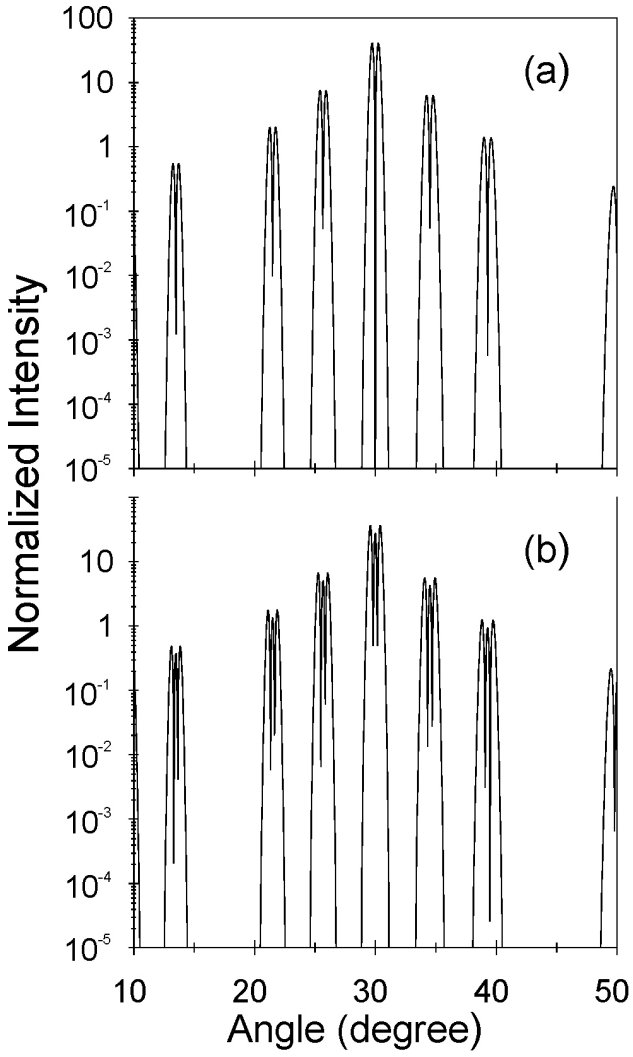

FIGURE 2. Diffraction patterns of Hermite-Gaussian beams at the angle of incidence $\theta_i = 30°$ for $m = 1, 2$, when $\ell_1 = 0.5$, $\ell_2 = 1.0$, $L = 10/\sqrt{2}$, $\lambda = 0.1$, and $(b, h) = (20.0, 4.0)$.

and the power ratio P given by

$$P = P_{\min}/P_{\max} \quad (13)$$

for a Ronchi ruling of period $d = \ell_1 + \ell_2$, where $P_{\min}$ and $P_{\max}$ are the minimum and maximum transmitted power, and $E_{\min}$ and $E_{\max}$ are the minimum and maximum values of the normally diffracted energy $I(0^0)$.

It is interesting to know the influence of the width of the opaque zone (ℓ_1) and transparent zone (ℓ_2) on the intensity ratio K and the power ratio P. For this, in Fig. 3 and Fig. 4 the ratios P and K are plotted, respectively, as a function of the parameter $q = \ell_1/\ell_2$, for $0.066 \leq q \leq 15$. We assume a normally incident Gaussian beam on the Ronchi ruling, with $L = 450/\sqrt{2}$ μm, $d = 320$ μm, and $\lambda = 0.633$ μm. From these figures, we find that K and P have a monotone decreasing behavior when $q = \ell_1/\ell_2$ is increased.

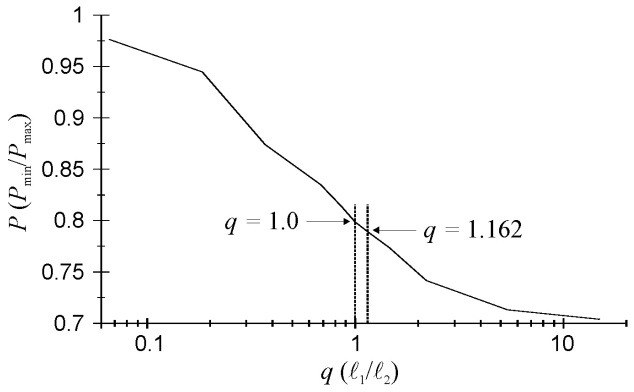

FIGURE 3. The power ratio P is plotted as a function of the parameter $q = \ell_1/\ell_2$. We assume a normally incident Gaussian beam on the Ronchi ruling, with $L = 450/\sqrt{2}$ μm, $d = 320$ μm, and $\lambda = 0.633$ μm.

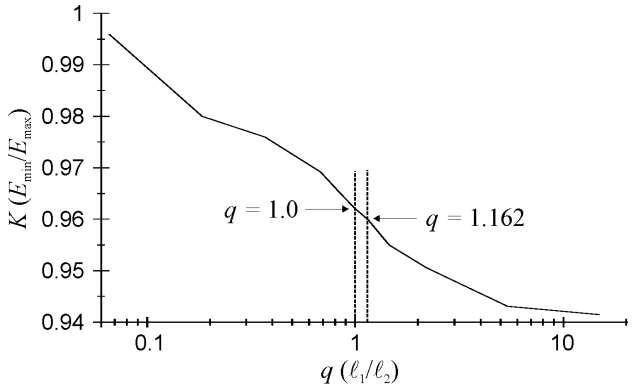

FIGURE 4. The intensity ratio K is plotted as a function of the ratio $q = \ell_1/\ell_2$. Same parameters as in Fig. 3.

In both figures, the results for an ideal Ronchi ruling are indicated with $q = 1.0$, and also the results for $q = 1.162$ are shown. For these particular cases, the values obtained are very similar; in fact, we have found that the relative error between both results is better than 1.2%. This conclusion will be important in the section on experimental results.

4. Definitions of Gaussian beam width

As noted in Ref. 3, the most common definition of width for a Gaussian mode TEM_{00} is given by the width at which the beam intensity drops to $1/e^2$ of the peak value. This value is denoted by $L_{e^{-2}}$. However, when the intensity drops to $1/e$ is also used and the corresponding beam width will be denoted by L. In particular, in this paper the value $1/e$ will be used from here on.

We assume the following intensity distribution of the incident Gaussian beam

$$I(x) = I_p \exp[-4x^2/L^2], \tag{14}$$

where $I(x)$ is the intensity as a function of the coordinate x, I_p is the peak intensity at the center of the beam, and L is the beam width.

There are other definitions based on the energy enclosure [3]. For instance, the beam width can be calculated using the diameter that passes 86.5% of the energy, in this case the beam width will be denoted by $L_{86.5}$. As was pointed in Ref. 14 the relationship between L and $L_{86.5}$ is given by means of the linear relationship $L_{86.5} = 1.057L$.

5. Two beam width methods

Now we go on to establish the two methods used with a Ronchi ruling in order to determine the Gaussian spot size. But before this, it is necessary to consider the Ronchi ruling utilized in the experimental set up in the next section. In the real grating used, the transparent and opaque zones have different widths, 148 μm and 172 μm, respectively. Then, for this grating we have $q = 1.162$ with the period given by $d = 320$ μm. In addition, we have a He-Ne laser operating at 633nm. Then, from the last result of Sec. 3.2, we conclude that the results obtained with this grating and those obtained from an ideal Ronchi ruling with $q = 1.0$ will be very similar.

In Fig. 5, the intensity ratio K and the power ratio P are plotted as functions of the normalized beam width L/ℓ_2 for a Ronchi ruling of period d. These results of K and P are given for $\ell_1 = 172$ μm and $\ell_2 = 148$ μm; however, from the considerations given above, these results are very similar to those given in Fig. 3 of Ref. 11 for $q = 1.0$.

We mention two important facts. Firstly, the results given in Fig. 5 are independent of the wavelength. Secondly, we have verified that the values of P are identical to those obtained for a two-dimensional Gaussian beam [6] when the spot is displaced normally to the slits. From these facts we can conclude that the results of Fig. 5 provide us with a method for determining the beam width.

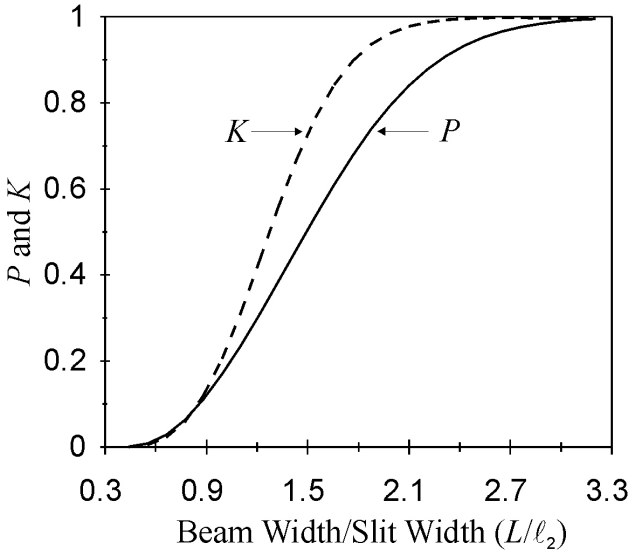

FIGURE 5. Intensity ratio $K = E_{\min}/E_{\max}$ (dashed curve) and power ratio $P = P_{\min}/P_{\max}$ (solid curve) as functions of the normalized beam width L/ℓ_2, for a Ronchi ruling with $q = 1.162$.

From Fig. 5 we get that the behavior of P and K are very similar but not identical, and that the beam width L can be determined as long as $0.2 < L/d < 1.5$, where d is the period of the ruling. The beam width L determined by P- and K-graphs will be denoted by L_{power} and $L_{I(0)}$, respectively.

6. Experimental set-up

A He-Ne laser operating at 633nm gives a TEM_{00} beam of diameter of about 1mm. This beam was passed through a linear polarizer in order not to saturate a RCA 30807 silicon detector. After the polarizer, the beam was propagated 6.5 cm and it was passed through a lens of focal length 25 cm. The experimental configuration is illustrated in Fig. 6.

The Ronchi ruling was placed at eight locations in the vicinity of the lens focus. The Ronchi ruling used was an Edmond Scientific ruling of period $d = 320$ μm. The set of distances between the lens and the Ronchi ruling are given by z =15 cm, 17.5 cm, 20 cm, 22.5 cm, 25 cm, 27.5 cm, 30 cm, and 32.5 cm.

The detector was fixed at a distance Q =10 cm for the power method and at Q =1.43 m in order to determine the normally diffracted energy $I(0^0)$. The detector scanned the beam wave normaly with a resolution given by 1100 steps by 1 mm. The signal provided by this detector and its lateral displacement was processed and controlled with a LabView program.

7. Comparison of the two methods

The experimental results obtained when the beam wave is scanned by the Ronchi ruling at the position z =22.5 cm are given in Fig. 7. We have plotted the total transmitted power as a function of the position. Also, in this figure we have added the theoretical results obtained by means of Eq. (10). In this case the experimental power method gives the beam width $L_{\text{power}} = 0.168$ mm.

The observed discrepancy between the theoretical and experimental results may be the consequence of several sources of error such as the non-uniform movement of the detector and the fact that the beam emitted by the laser is not a truly Gaussian beam.

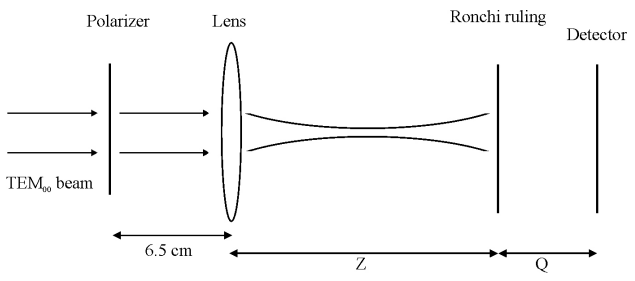

FIGURE 6. Our experimental configuration.

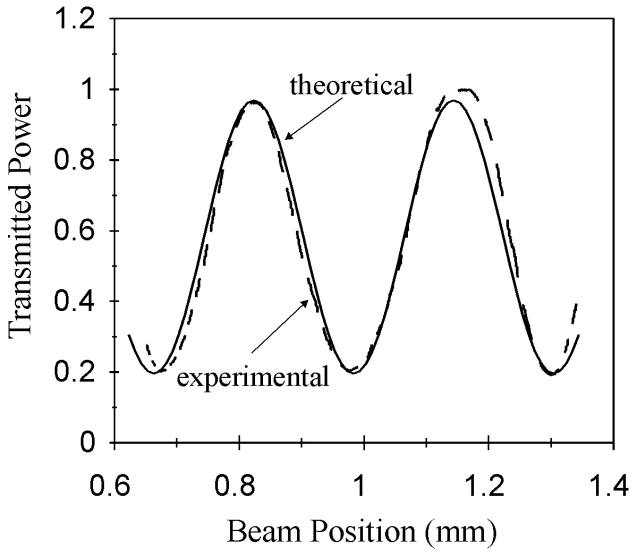

FIGURE 7. Transmitted power (arbitrary units) as a function of the beam position when the Gaussian beam wave is scanned by the Ronchi ruling at z =22.5 cm. a) Experimental results (dashed curve) and b) theoretical results (solid curve).

In Fig. 8, the normally diffracted energy $I(0^0)$ obtained experimentally is given as a function of the beam position, and also for z =22.5 cm as in Fig. 7. The proposed method gives the beam width $L_{I(0)} = 0.157$ mm. Note that the relative error between L_{power} and $L_{I(0)}$ is 6.54%. In the same figure we have compared the experimental results with those obtained by means of Eq. (9).

In Fig. 9, the beam widths obtained with the two methods are plotted as functions of the distance z between the lens and the Ronchi ruling. We observe that the results obtained with the two Ronchi ruling methods are very close. We conclude that the two analyzed methods, which do not produce identi-

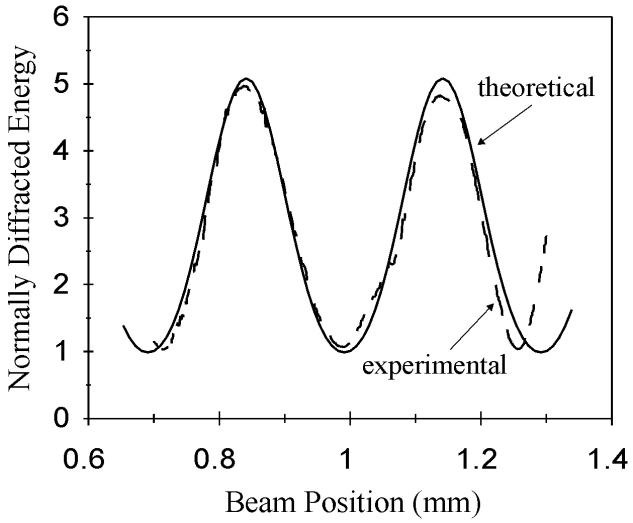

FIGURE 8. Normally diffracted energy (arbitrary units) as a function of the beam position when the Gaussian beam is scanned by the Ronchi ruling at $z = 22.5$ cm. a) Experimental results (dashed curve) and b) theoretical results.

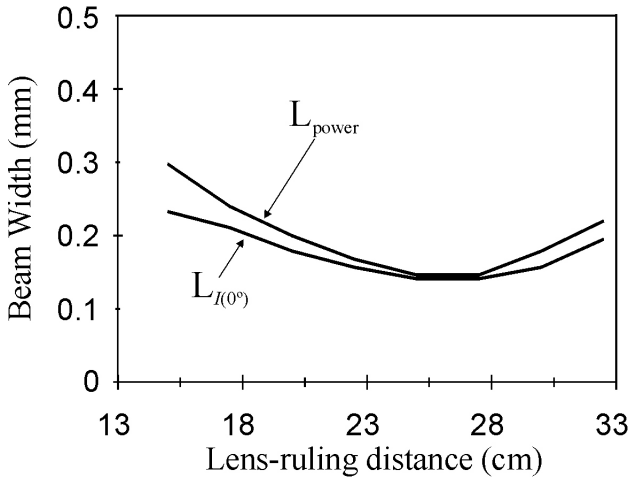

FIGURE 9. The beam width obtained with the two methods as a function of the distance z between the lens and the Ronchi ruling.

cal results, are sufficiently close to be useful in the determination of the Gaussian beam diameters. To our knowledge, this is the first time that these two Ronchi methods are confronted with the experiment. It is interesting to observe Fig. 4 of Ref. 3, where the beam width is measured by means of four methods, the knife edge method, the slit method, a method based on the second moment or variance, and the so-called TEM_{00} method.

8. Conclusions

Two independent methods for Gaussian spot size measurement based on a Ronchi ruling are experimentally compared. One of them considers the total transmitted power, and the other one the normally diffracted energy. To our knowledge, the two methods had not been tested previously by experiment. We show that the beam widths obtained by the two methods are very close.

Acknowledgment

The authors acknowledge support from Comisión de Operaciones y Fomento de Actividades Académicas del Instituto Politécnico Nacional.

1. D. Psaltis, D.G. Stinson, and G.S. Kino, *Optics&Photonics News* **November** (1997) 35.
2. R.M. Herman, J. Pardo, and T.A. Wiggins, *Appl. Opt.* **24** (1985) 1346.
3. D. Wright, *Opt. and Quantum Electr.* **24** (1992) S1129.
4. O. Mata-Mendez, *Opt. Lett.* **16** (1991) 1629.
5. N. Hodgson, T. Haase, R. Kostka, and H. Weber, *Opt. and Quantum Electr.* **24** (1992) S927.
6. M.A. Karim *et al.*, *Opt. Lett.* **12** (1987) 93.
7. A.K. Cherri, A.A.S. Awwal, and M.A. Karim, *Appl. Opt.* **32** (1993) 2235.
8. A.A.S. Awwal, J.A. Smith, J. Belloto, and G. Bharatram, *Opt. and Laser Thechn.* **23** (1991) 159.
9. A.K. Cherri, A.A.S. Awwal, *Optical Engineering* **32** (1993) 1038.
10. J.S. Uppal, P.K. Gupta, and R.G. Harrison, *Opt. Lett.* **14** (1989) 683.
11. O. Mata-Mendez and F. Chavez-Rivas, *J. Opt. Soc. Am. A* **18** (2001) 537.
12. L.E. Regalado, V. Bredart, and J. Sandoval Chávez, *Rev. Mex. Fís.* **41** (1995) 882.
13. A. Sommerfeld, "Optics" in *Lectures on Theoretical Physics* Vol.IV, Chap. VI (Academic, New York, 1964) 273.
14. O. Mata-Mendez and F. Chavez-Rivas, *J. Opt. Soc. Am A* **12** (1995) 2440.
15. H. Laabs and B. Ozygus, *Opt. Laser Technol.* **28** (1996) 213.